

Activation of Nickel–Chromium Hydrogenation Catalysts with Hydrogen

I. I. Simentsova^{a,*}, N. V. Shtertser^{a,b}, L. M. Plyasova^a, T. P. Minyukova^a, and T. M. Yurieva^a

^a *Borckov Institute of Catalysis, Siberian Branch, Russian Academy of Sciences, Novosibirsk, 630090 Russia*

^b *Novosibirsk State University, Novosibirsk, 630090 Russia*

**e-mail: sii@catalysis.ru*

Received March 21, 2015

Abstract—The kinetics of the reduction of nickel cations in nickel oxide and nickel–chromium catalysts whose oxide precursors have different structures has been investigated by thermal analysis. The reduction of nickel oxide with a hydrogen-containing gas takes place at 250–330°C. The apparent activation energy of this reaction is about 88 kJ/mol. The introduction of up to 30 at % chromium cations into the nickel oxide structure shifts the reduction temperature of nickel in the oxide phase to 300–450°C and increases the apparent activation energy of the reduction of nickel cations to ~108 kJ/mol. The introduction of 67 at % chromium into nickel oxide results in the formation of an oxide precursor with a spinel structure. The apparent activation energy of the reduction of nickel cations in this spinel is about 163 kJ/mol. The results of this study can be used in optimizing the composition of Ni-containing hydrogenation catalysts and their activation and operation conditions.

Keywords: NiCr catalysts, nickel oxide, spinel, reductive activation

DOI: 10.1134/S0023158416020130

INTRODUCTION

Nickel-containing compounds are widely used as catalysts in the hydrogenation of organics and carbon oxides [1–5]. Prior to being employed in a hydrogenation reaction, the catalysts are activated with a hydrogen-containing gas. The activity of such systems is determined by the presence of ~2–10 nm nickel metal particles [6–8]. The activity and selectivity of the catalysts in hydrogenation reactions is known to depend significantly on the structure of their hydroxo precursors and on the conditions under which the precursors were heat-treated [9]. However, it is still unclear how the kinetics of the reduction of nickel-containing catalysts depends on the composition and structure of their oxide precursors.

In this study, we obtained precursors having the cubic structure of nickel oxide and nickel–chromium spinel and investigated the reduction of nickel cations in nickel oxide and nickel–chromium oxide catalysts. The activation energies of the reduction of nickel cations in structurally different oxide precursors were estimated.

EXPERIMENTAL

Sample Preparation

Oxide precursors were obtained by heat treatment of mixed hydroxo compounds in flowing argon. The hydroxo compounds were synthesized by the continuous coprecipitation of nickel and chromium cations

from aqueous solutions of nitrates at $T = 65\text{--}68^\circ\text{C}$ and pH 7.2–7.4. The nitrates— $\text{Ni}(\text{NO}_3)_2 \cdot 6\text{H}_2\text{O}$ (pure grade, USSR state standard *GOST 4055-78*) and $\text{Cr}(\text{NO}_3)_3 \cdot 9\text{H}_2\text{O}$ (pure grade, *GOST 4471-78*)—were received from the Ural Plant of Chemical Reagents. In the synthesis of catalysts with $\text{Ni}^{2+} : \text{Cr}^{3+} = 1 : 0$ (no chromium) and 2.3 : 1, the precipitant was sodium carbonate; ammonium carbonate was used in the preparation of the $\text{Ni}^{2+} : \text{Cr}^{3+} = 1 : 2$ sample. The precipitates were washed to remove sodium ions (down to a level of ≤ 0.01 wt %) and ammonium nitrate traces, dried under an IR lamp at $T \approx 50\text{--}60^\circ\text{C}$, and calcined at 400 and 600–650°C in flowing argon. Calcination was performed to rule out the oxidation of Cr^{3+} to Cr^{6+} .

The cationic composition of the synthesized samples was verified by atomic emission spectroscopy (AES). Table 1 lists the designations and chemical compositions of the samples synthesized.

Physicochemical Methods of Characterization of Samples

X-ray diffraction (XRD) patterns were obtained on a D-500 diffractometer (Siemens, Germany) using monochromatic $\text{CuK}\alpha$ radiation with a monochromator placed in the reflected beam. The diffraction patterns were recorded at $2\theta = 10^\circ\text{--}70^\circ$ with 0.05° increments. The counting time per data point was 5 s.

Table 1. Designation and chemical composition of the materials examined

Sample	Ni ²⁺ : Cr ³⁺ ratio	Chemical composition in atomic fractions
Ni1	1 : 0	Ni _{1.0} Cr _{0.0}
NiCr2.3	2.3 : 1	Ni _{0.70} Cr _{0.30}
NiCr0.5	1 : 2	Ni _{0.33} Cr _{0.67}

Differential thermogravimetric (DTG) analyses were carried out using a Netzsch STA-409 PC Luxx thermoanalytical system (Netzsch, Germany). The samples were reduced in the temperature-programmed mode in an H₂ : Ar = 50 : 50 (vol %) mixture flowing at a rate of 80 mL/min. The temperature was elevated at a rate of 5, 7, or 10°C/min. The samples to be examined were pre-heat-treated at 400°C in flowing argon. In the preparation of Ni-containing catalysts, the pre-heat-treatment temperature is often chosen to be 400°C, so it was of greatest interest to study the samples prepared at this very temperature. A 30- to 50-mg catalyst sample was placed in a platinum crucible. TGA data were processed using the standard single-point method ASTM E 698 [10].

RESULTS AND DISCUSSION

The XRD patterns of the Ni–Cr samples calcined at 400°C in flowing argon (Fig. 1, curves 1–3) show three diffuse maxima at $2\theta \approx 36, 43,$ and 62 deg, which are assignable to an fcc phase. However, as judged from the distribution of reflection intensities, the samples differ in their structure. For the NiCr2.3 sample, the strongest reflection is the one that occurs at $2\theta \approx$

$42\text{--}43$ deg and the three observed reflections are assignable to a NaCl–NiO type structure and can be given the indexes 111, 200, and 220. The corresponding unit cell parameter a is ~ 4.186 Å (± 0.003 Å), slightly larger than the reference unit cell parameter for pure NiO ($a = 4.177$ Å, see ICDD PC-WIN, PDF-2, 00-047-1049). This is evidence that the structure is disordered due to the fact that its octahedral oxygen-surrounded sites are occupied not only by Ni²⁺ cations but also by Cr³⁺ cations. For the NiCr0.5 sample, the strongest reflection is that occurring at $2\theta \approx 36^\circ$ ($d_{\max}^{311} \approx 2.4\text{--}2.5$ Å), which is characteristic of the spinel structure. The unit cell parameter of this spinel is ~ 0.05 Å larger than the reference value for NiCr₂O₄ ($a = 8.320$ Å see ICDD PC-WIN, PDF-2, 00-023-1271). These oxide structures are sometimes referred to as anion-modified structures [11] and, in some works, protospinel [12]. These structures contain impurity anions hampering their crystallization and are characterized by an incomplete spinel-type diffraction pattern with an increased unit cell parameter. Raising the heat treatment temperature leads to the ordering of the cation distribution and to the formation of a normal spinel structure.

Calcination in argon at 600–650°C (Fig. 1, curves 4, 5) increases the proportion of crystalline phases in the samples. The NiCr0.5 sample, with a cation ratio of Ni²⁺ : Cr³⁺ = 1 : 2, which is characteristic of spinel-type oxide phases, consists mainly of the nickel–chromium spinel phase and contains some amount of the nickel oxide phase. The NiCr2.3 sample is the nickel oxide phase containing a minor amount of nickel–chromium spinel.

The thermoanalytical data for the oxide samples heat-treated at 400°C in flowing argon are presented in Figs. 2–4. Figure 2 shows DTG profiles for the reduction of chromium-free nickel oxide that were recorded at different heating rates. This sample was precalcined in the chamber of the thermal analyzer at 400°C in flowing argon and was then reduced in situ under anaerobic conditions. The thermoanalytical profiles for the reduction of the sample under these conditions show no peaks assignable to the elimination of adsorbed or weakly bonded water. It can be seen in Fig. 2 that the reduction of nickel in nickel oxide takes place in a single step. The weight loss rate maximum shifts from 275 to 293°C as the heating rate is increased from 5 to 10°C/min. About 20% of the sample weight is lost here.

The DTG profiles for the oxide sample NiCr2.3 precalcined at 400°C in argon, recorded at three different temperature ramp rates (5, 7, and 10°C/min), are shown in Fig. 3. It is clear that the conversion of the NiCr2.3 sample being heat-treated with the hydrogen-containing mixture occurs in two stages. The first stage shows itself as a slight (2–3%) weight loss. The extremum of the corresponding peak shifts from ~ 116 to $\sim 136^\circ\text{C}$ as the temperature ramp rate is

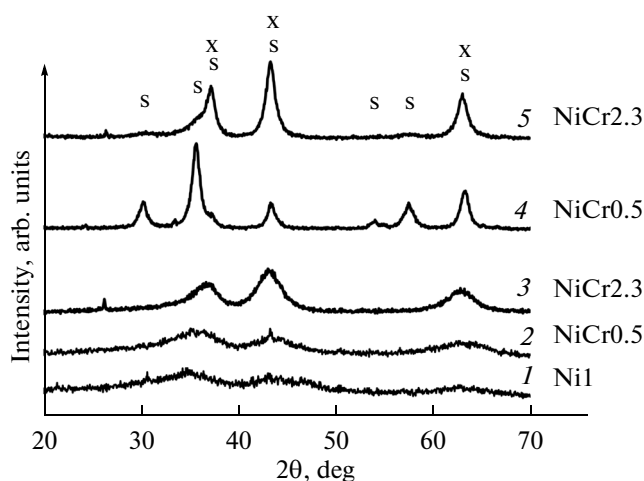


Fig. 1. X-ray diffraction patterns of the nickel–chromium samples calcined in flowing argon at (1–3) 400 and (4, 5) 600–650°C: x, NiO phase; s, spinel phase (NiCr₂O₄).

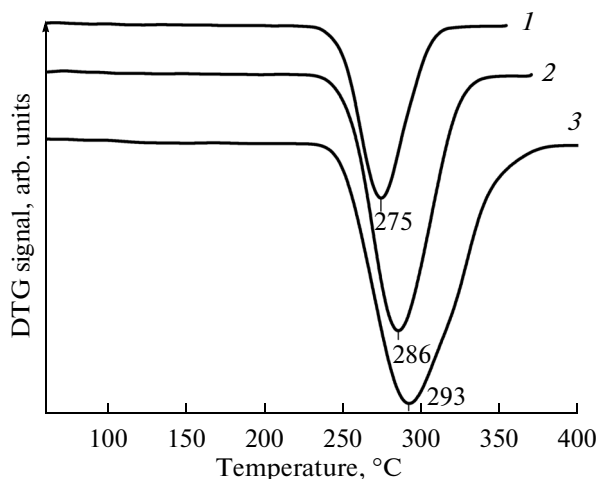


Fig. 2. DTG profiles for the reduction of the Ni1 sample (400°C, argon) in the hydrogen-containing medium at a heating rate of (1) 5, (2) 7, and (3) 10°C/min. H₂ : Ar = 50 : 50 vol %.

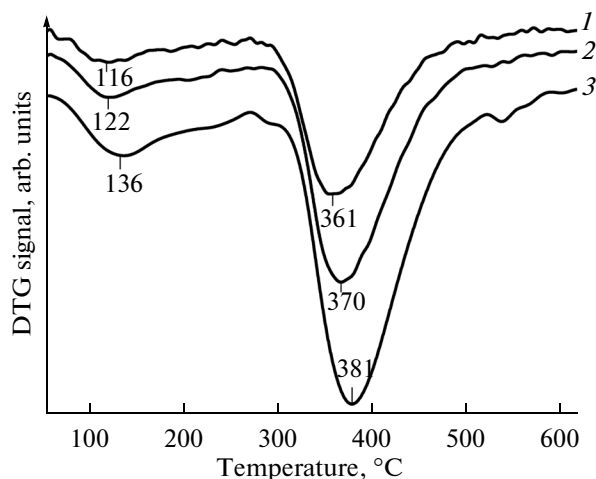


Fig. 3. DTG profiles for the reduction of the NiCr2.3 sample (400°C, argon) in the hydrogen-containing medium at a heating rate of (1) 5, (2) 7, and (3) 10°C/min. H₂ : Ar = 50 : 50 vol %.

increased from 5 to 10°C/min. This conversion of the sample involves loss of adsorbed and weakly bound water. The second stage of the process is the reduction of nickel cations in the nickel–chromium oxide, which is accompanied by a weight loss of about 14%. The position of the weight loss rate maximum shifts from 361 to 381°C with an increasing heating rate.

Note that the reduction of nickel cations in the sample that contains 30 at % chromium and has a nickel oxide type structure occurs at a 90°C higher temperature than the same process in pure nickel oxide. The single-step reduction of this material is evidence that it is dominated by the nickel oxide phase.

Figure 4 shows the thermoanalytical profiles characterizing the reduction of the NiCr0.5 sample. Along with the elimination of adsorbed and weakly bound water at ~118–135°C, there are two nickel reduction events manifesting themselves as weight loss rate maxima in the temperature ranges from 239 to 259°C and from 416 to 432°C. The positions of these maxima depend on the temperature ramp rate, which was varied between 5 and 10°C/min. The weight lost by the sample below 300°C corresponds to the reduction of ~10% of the nickel cations. Above 350°C, ~90% of the nickel cations in the catalyst undergo reduction. This reduction behavior indicates that the sample contains two nickel-containing oxide phases. The main event occurring above 350°C is nickel reduction in the spinel phase. The thermal event taking place at 239–259°C is nickel reduction in the NiO-type phase.

Thus, the XRD and DTG data demonstrated that the introduction of up to 30 at % chromium into the NiCr oxide sample does not alter the NiO-type structure, while the introduction of 67 at % chromium yields a material dominated by an oxide phase with a nickel–chromium spinel structure.

Table 2 presents weight loss data derived for the samples examined from TG curves for nickel reduction (Δm) at the three temperature ramp rates and is supplemented by calculated weight loss data (Δm^{calc}) corresponding to complete nickel reduction in the catalysts. Clearly, the experimental weight loss data are in good agreement with the data calculated for the reduction of 100% of the nickel cations in the catalyst samples.

Table 2 also presents apparent activation energy (E_a) data for the reduction of nickel cations to Ni⁰. The activation energies were determined using DTG peak temperatures at different heating rates. These

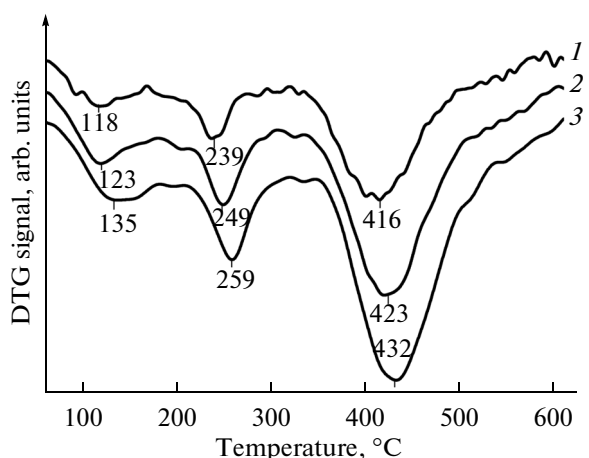


Fig. 4. DTG profiles for the reduction of the NiCr0.5 sample (400°C, argon) in the hydrogen-containing medium at a heating rate of (1) 5, (2) 7, and (3) 10°C/min. H₂ : Ar = 50 : 50 vol %.

Table 2. Weight loss data pertaining to nickel cation reduction for the nickel-containing catalysts*

Sample	T_{\max} , °C			Δm , %			Δm_{calc} , %	E_a , kJ/mol
	heating rate, °C/min			heating rate, °C/min				
	5	7	10	5	7	10		
Ni1	275	286	293	20.6	20.8	20.7	21.4	88
NiCr2.3	361	370	381	14.5	14.6	14.6	14.9	108
NiCr0.5	416	423	432	6.3	6.5	6.4	7.1	163

* Gas mixture: H_2 : Ar = 50 : 50 vol %.

calculations were performed using an equation of the standard single-point method ASTM E 698:

$$\ln\left(\frac{\beta_j}{T_{j,\max}^2}\right) = -\frac{E}{RT_{j,\max}}, \quad (1)$$

where $T_{j,\max}$ is the peak temperature at the heating rate β_j .

Figure 5 presents experimental kinetic data fitted to Eq. (1).

The apparent activation energies of the reduction of nickel cations in nickel oxide and NiCr2.3 are ~88 and ~108 kJ/mol, respectively (Fig. 5). For NiCr0.5, the calculated E_a value is considerably higher and is ~163 kJ/mol. Therefore, the reduction of nickel cations in the NiO-type oxide phase is characterized by a much lower activation energy than the same process in the spinel-type oxide phase.

Thus, the nickel–chromium oxide catalysts with $\text{Ni}^{2+} : \text{Cr}^{3+} = 1 : 0, 2.3 : 1, \text{ and } 1 : 2$ differ in how their nickel cations are reduced. It was demonstrated that nickel oxide reduction in the hydrogen-containing gas occurs at 250–330°C with an E_a of about 88 kJ/mol. The introduction of up to 30 at % chromium cations into the nickel oxide structure increases the temperature of nickel reduction in the nickel oxide phase to 300–450°C and raises the apparent E_a of nickel cation reduction to ~108 kJ/mol. At a higher chromium content of 67 at %, a spinel-type oxide precursor forms, for which the apparent activation energy of nickel cation

reduction is about 163 kJ/mol. The results of this study can be used in optimizing the composition and activation and operation conditions for nickel-containing hydrogenation catalysts.

ACKNOWLEDGMENTS

This study was supported by the Russian Foundation for Basic Research, project no. 13-03-00469.

REFERENCES

- Rodrigo, M.T., Daza, L., and Mendioroz, S., *Appl. Catal., A*, 1992, vol. 88, p. 101.
- Enger, B.Ch. and Holmen, A., *Catal. Rev. Sci. Eng.*, 2012, vol. 54, p. 437.
- Veldsink, J.W., Bouma, M.J., Schoon, N.-H., and Beenackers, A.A.C.M., *Catal. Rev. Sci. Eng.*, 1997, vol. 39, p. 253.
- Louloudi, A., Michalopoulos, J., Gangas, N.-H., and Papayannakos, N., *Appl. Catal. A*, 2003, vol. 242, p. 41.
- Minyukova, T.P., Itenberg, I.Sh., Khassin, A.A., Sipatrov, A.G., Dokuchits, E.V., Terentiev, V.Ya., Khristolyubov, A.P., Brizitskii, O.F., and Yurieva, T.M., *J. Chem. Eng.*, 2007, vol. 134, p. 235.
- Bitter, J.H., Lee, M.K., Slotboom, A.G.T., Dileen, A.J., and Jong, K.P., *Catal. Lett.*, 2003, vol. 89, p. 139.
- Molina, R. and Poncelet, G., *J. Catal.*, 2001, vol. 199, p. 162.
- Boudart, M. and Conica, C.M.M., *J. Catal.*, 1989, vol. 117, p. 33.
- Simentsova, I.I., Minyukova, T.P., Khassin, A.A., Dokuchits, E.V., Davydova, L.P., Molina, I.Yu., Plyasova, L.M., Kustova, G.N., and Yurieva, T.M., *Russ. Chem. Bull.*, 2010, vol. 59, No 11, p. 2055.
- Kissinger, H.E., *J. Res. Nat. Bur. Stand.*, 1956, vol. 57, p. 217.
- Litvak, G.S., Minyukova, T.P., Demeshkina, M.P., Plyasova, L.M., and Yurieva, T.M., *React. Kin. Cat. Lett.*, 1986, vol. 31, p. 403.
- Erenburg, B.G., Fateeva, V.P., Likhovid, L.I., and Min'kov, A.I., *Izv. Sib. Otd. Akad. Nauk SSSR*, 1981, no. 2, p. 51.

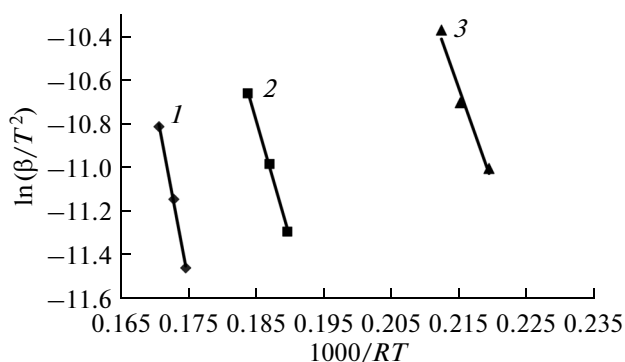


Fig. 5. Experimental kinetic data represented in the coordinates of Eq. (1) for nickel reduction in the (1) NiCr0.5, (2) NiCr2.3, and (3) Ni1 catalysts.

Translated by D. Zvukov